Alexandria Engineering Journal (2022) 61, 1996–2008

HOSTED BY
ELSEVIER

Alexandria University

Alexandria Engineering Journal

www.elsevier.com/locate/aej
www.sciencedirect.com

On beta-time fractional biological population model with abundant solitary wave structures

Kottakkaran Sooppy Nisar [a,*], Armando Ciancio [b], Khalid K. Ali [c], M.S. Osman [d,e,*], Carlo Cattani [f], Dumitru Baleanu [g,h,l], Asim Zafar [i], M. Raheel [j], M. Azeem [k]

[a] Department of Mathematics, College of Arts and Sciences, Wadi Aldawaser 11991, Prince Sattam bin Abdulaziz University, Saudi Arabia
[b] Department of Biomedical and Dental Sciences and Morphofunctional Imaging, University of Messina, Messina, Italy
[c] Mathematics Department, Faculty of Science, Al-Azhar University, Nasr-City, Cairo, Egypt
[d] Department of Mathematics, Faculty of Science, Cairo University, Giza 12613, Egypt
[e] Department of Mathematics, Faculty of Applied Science, Umm Alqura University, Makkah 21955, Saudi Arabia
[f] Engineering School, DEIM, Tuscia University, Viterbo, Italy
[g] Department of Mathematics, Faculty of Arts and Sciences, Çankaya University, Ögretmenler Cad. 1406530, Ankara, Turkey
[h] Institute of Space Sciences, Magurele, Bucharest, Romania
[i] Department of Mathematics, CUI Vehari Campus, Pakistan
[j] Department of Mathematics & Statistics, ISP Multan, Pakistan
[k] Department of Mathematics & Statistics, The University of Lahore, Pakistan
[l] Department of Physics, University of Craiova, Romania13 A.I.Cuza, 200 585 Craiova, Romania

Received 26 December 2020; revised 26 May 2021; accepted 14 June 2021
Available online 11 August 2021

KEYWORDS

Biological population model;
Novel derivative operator;
Solitons;
Finite difference method

Abstract The ongoing study deals with various forms of solutions for the biological population model with a novel beta-time derivative operators. This model is very conducive to explain the enlargement of viruses, parasites and diseases. This configuration of the aforesaid classical scheme is scouted for its new solutions especially in soliton shape via two of the well known analytical strategies, namely: the extended Sinh-Gordon equation expansion method (EShGEEM) and the Exp_a function method. These soliton solutions suggest that these methods have widened the scope for generating solitary waves and other solutions of fractional differential equations. Different types of soliton solutions will be gained such as dark, bright and singular solitons solutions with certain conditions. Furthermore, the obtained results can also be used in describing the biological population model in some better way. The numerical solution for the model is obtained using the finite difference method. The numerical simulations of some selected results are also given through their physical explanations. To the best of our knowledge, No previous literature discussed this model through the application of the EShGEEM and the Exp_a function method and supported their

* Corresponding authors at: Department of Mathematics, College of Arts and Sciences, Wadi Aldawaser 11991, Prince Sattam bin Abdulaziz University, Saudi Arabia (K. S. Nisar). Department of Mathematics, Faculty of Science, Cairo University, Giza 12613, Egypt (M.S. Osman).
E-mail addresses: n.sooppy@psau.edu.sa (K.S. Nisar), mofatzi@sci.cu.edu.eg (M.S. Osman).
Peer review under responsibility of Faculty of Engineering, Alexandria University.

https://doi.org/10.1016/j.aej.2021.06.106

new obtained results by numerical analysis.

1. Introduction

In this world, human life affected due to the changes occur on the earth. World with its medley from smooth to persuasive is adequate of interactions. Many natural phenomenon are occurring in this universe [1–4]. To understand these phenomenon soliton theory is very helpful in various fields. Likely, soliton theory is used in the field of applied physics. Regarding this issue, many researchers investigated their works by solving a variety of nonlinear partial differential equations (NLPDEs).

Different analytical schemes are constructed to deal with these NLPDEs. In [5], two kinds of bright solitons have been found for the perturbed Gerdjikov-Ivanov (PGI) model by applying the semi-inverse variational technique. Various solitons of new coupled evolution equation are explained [6]. The unified, the generalized unified and the Hirota methods are used to find single wave and multi-wave solutions for different models in many branches of science [7–12]. Periodic soliton solutions are discussed by accomplishing the variational principle algorithm for the Kundu-Mukherjee-Naskar model in the 2D form [13]. Riccati equation method is used to investigate some optical soliton solutions in the fiber communication system [14]. For more, see [15–34].

The objective of this work is to determine the solutions of the degraded parabolic model appearing in the 3D diffusion of biological populations:

$$\frac{\partial}{\partial t}q(x,y,t)=\frac{\partial^2}{\partial x^2}(q^2(x,y,t))+\frac{\partial^2}{\partial y^2}(q^2(x,y,t))+F(q(x,y,t)),\quad t\geqslant 0,\quad x,y\in\Re. \tag{1}$$

Biologists consider that enlargement or desertion perform a basic aspect in the reorganization of population of some sorts. The pervasion of this model in a certain domain Ω is explained by the following functions in position and time [35]:

$q(\Im,t)$, the population density,

$F(\Im,t)$, population accumulation, where $\Im=\Im(x,y)$.

$q(\Im,t)$ represents the individuals number in its arguments while the total population of Λ at t is represented by its integral over any sub-region Λ. The population flux from position to other is defined by the diffusion velocity $\upsilon(\Im,t)$. In [35], a certain transformation is investigated to reduce Eq. (1) to another one that existed in the porous media theory. Thus, it verified the theorems of existence and uniqueness for the initial-value problem in one-dimensional besides the solution for an initial point source. According to the law of population balance, for any regular sub-region Λ of Ω and time t, the fields q,υ and F are constants:

$$\frac{d}{dt}\int_\Lambda q dV+\int_{\partial\Lambda} q\mathbf{v}.n dA=\int_\Lambda F dV, \tag{2}$$

n here represents unit normal outwards from the boundary $\partial\Lambda$ to Λ. Eq. (2) indicates that the sum of the rate of change of population of Λ and the rate at which individuals leave Λ through its boundary is equivalent to the rate at which individuals are accumulated directly to Λ.

Gurtin and Maccamy in [35] exhibited that by deciding the hypothesis

$$F=F(q),\quad \upsilon=-\mho(q)\nabla q, \tag{3}$$

where $\mho(q)>0$ for $q>0$. So, we get:

$$q_t=P(q)_{xx}+P(q)_{yy}+F(q),\quad t\geqslant 0,\quad x,y\in\Re, \tag{4}$$

where $P=P(q)$ is a function in q and some particular cases of it are investigated by Gurney and Nisbet [36]. They discussed it in the animals population. The motions are made mostly either by young animals reaching maturity and evacuating out of their parental region to settle down nurturing territory of their own, or by mature animals expelled out by invaders. In the previous statuses, they will be directed toward nearby unoccupied territory. Herein, movement will appear almost down the population density gradient, and it will be more active at higher densities of population. In an endeavor to paradigm this condition, they needed a walk through a rectangular grid in which an animal can either remain at its current position or go out in the direction of lowest population density. The probability distribution in these two situations is determined by the magnitude of the gradient of the population density at the appropriate grid location. When $P(q)=q^2$, our model can be written as

$$q_t=q^2_{xx}+q^2_{yy}+F(q), \tag{5}$$

where $q=q(x,y,t)$ shows the population density function and $F(q)$ indicates the population accumulation due to births and deaths. Few characteristics of the above Eq. (5) like Hölder measurements of its solutions are explained in [38]. $F(q)$ has different forms with different meanings given as follow:

The Malthusian law $F(q)=\mu q$ here μ is constant.

The Verhulst law $F(q)=\mu q-\tau q^2$ where μ,τ are constants.

Let's consider the new form of the F as the $F(q)=\sigma(q^2-\rho)$, which gives

$$q_t=q^2_{xx}+q^2_{yy}+\sigma(q^2-\rho), \tag{6}$$

where σ and ρ are the constants.

This biological population model is very helpful to explain the enlargement of viruses, parasites and diseases. On the basis of this model, the greatest harvest for farmers can be found. Biological population model can tread the delicate species and work and control their devolution.

This model have been solved by different analytical methods such as: dark traveling wave solution has been determined by applying the anstaz method [37], different exact soliton solutions has been determined by implementing the exp-function scheme [39], hyperbolic and trigonometric type soliton solutions has been found with the use of (G'/G)–Expansion technique [40], by using modified exp-function scheme explicit solitons of this model has been obtained in [41], various exact wave solitons of this model obtained by utilizing the Adomian's decomposition technique [42], exact and other types of soliton solutions of this model in time fractional form has been obtained by implementing the modified Exp-function method [43].

There are another two methods named as: the extended Sinh-Gordon equation expansion method (EShGEEM) and the Exp_a function method are applied to investigate the different types of wave solutions. Explicit solutions for the

Table 1 gives a comparison between the numerical results and the analytical solution in (25) when $\beta = 1, \rho = 0.05, \sigma = 0.005, \theta = 0.09, t = 0.01, k = 0.2, \Delta t = 0.001, h = 0.2$ and $y = 1$.

x	Numerical solution	Analytical solution	Absolute error
−2.0	0.244332	0.244332	0.00000
−1.4	0.244514	0.244514	7.88298 E-9
−1.0	0.244601	0.244601	7.97203 E-9
−0.4	0.244678	0.244678	8.05207 E-9
0.0	0.244695	0.244695	8.06876 E-9
0.4	0.244682	0.244682	8.05578 E-9
1.0	0.244609	0.244609	7.98119 E-9
1.4	0.244526	0.244526	7.89604 E-9
2.0	0.244349	0.244349	0.00000

Table 2 gives a comparison between the numerical results and the analytical solution in (25) when $\rho = 0.05, \sigma = 0.005, \theta = 0.09, t = 0.01, k = 0.2, \Delta t = 0.001, h = 0.2, x = 1$ and $y = 1$ with different values of β.

β	Numerical solution	Analytical solution	Absolute error
0.5	0.244612	0.244612	1.05792 E-8
0.6	0.244611	0.244611	9.33206 E-9
0.7	0.244609	0.244609	8.61447 E-9
0.8	0.244608	0.244608	8.21829 E-9
0.9	0.244606	0.244606	8.03016 E-9

Table 3 introduces a comparison between the numerical results and the analytical solution (44) when $b_0 = 0.01, b_1 = 0.02, a = 0.1, \rho = 0.1, \sigma = 0.1, \theta = 0.3, t = 0.01, k = 0.2, \Delta t = 0.001, h = 0.2$ and $y = 1$. Fig. 9 shows the results in Table 3.

x	Numerical solution	Analytical solution	Absolute error
−2.0	0.263168	0.263168	0.00000
−1.4	0.239776	0.239851	7.65690 E-5
−1.0	0.220171	0.220261	9.25751 E-5
−0.4	0.185347	0.185458	1.18125 E-4
0.0	0.160528	0.160648	1.34438 E-4
0.4	0.138198	0.138318	1.47989 E-4
1.0	0.121754	0.121836	1.57925 E-4
1.4	0.128496	0.128536	1.55148 E-4
2.0	0.158505	0.158505	0.00000

Table 4 introduces a comparison between the numerical results and the analytical solution (44) when $b_0 = 0.01, b_1 = 0.02, a = 0.1, \rho = 0.1, \sigma = 0.1, \theta = 0.3, \Delta t = 0.001, t = 0.01, k = 0.2, h = 0.2, x = 1$ and $y = 1$ with different values of β.

β	Numerical solution	Analytical solution	Absolute error
0.5	0.125814	0.125924	2.11285 E-4
0.6	0.124275	0.124372	1.85713 E-4
0.7	0.123286	0.123375	1.71045 E-4
0.8	0.122614	0.122699	1.62929 E-4
0.9	0.122129	0.122212	1.59027 E-4

Konopelchenko-Dubrovsky (KD) model in higher dimension have been determined by utilizing EShGEEM [44]. Distinct kinds of solitons like: dark, singular, bright and other solitons of conformable space–time fractional Fokas-Lenells equation have been studied by this method [45].

On the other hand, the Exp_a function method is a modern and simple way to obtain the exact rational solitons. This technique has been used to establish the exact solitons of combined KdV–mKdV equations [46]. Explicit exact solitons of two non-linear Schrödinger equations have investigated through two different techniques [47].

The main goal for this article is to find the optical solitons of the beta-time fractional biological population model equation based on the two different methods, the EShGEEM and the Exp_a function method. The numerical solution for this model will be introduced via the finite difference method.

2. β–time Derivative and it's properties

Definition: Suppose $g(\varsigma)$ is a function that is defined for all non-negative ς. Therefore, the beta-time fractional derivative can be defined as [48]

$$D^{\beta}(g(\varsigma)) = \frac{d^{\beta} g(\varsigma)}{d\varsigma^{\beta}} = \lim_{\epsilon\to 0}\frac{g(\varsigma+\epsilon(\varsigma+\frac{1}{\Gamma(\beta)})^{1-\beta})-g(\varsigma)}{\epsilon},\ \beta\in(0,1].$$

The main properties of the Beta-time fractional derivative are stated in the next theorem [48–53]:

Theorem: Assume $f(\varsigma)$ and $g(\varsigma)$ are the β-time differentiable functions $\forall\ \varsigma > 0$ and $\beta \in (0,1]$. Then

i. $D^{\beta}(af(\varsigma)+bg(\varsigma)) = aD^{\beta}(f(\varsigma)) + bD^{\beta}(g(\varsigma)), \forall a,b\in R.$

ii. $D^{\beta}(f(\varsigma)g(\varsigma)) = g(\varsigma)D^{\beta}(f(\varsigma)) + f(\varsigma)D^{\beta}(g(\varsigma)).$

iii. $D^{\beta}(\frac{f(\varsigma)}{g(\varsigma)}) = \frac{g(\varsigma)D^{\beta}(f(\tau))-f(\varsigma)D^{\beta}(g(\varsigma))}{(g(\varsigma))^2}.$

iv. $D^{\beta}(f(\varsigma)) = (\varsigma+\frac{1}{\Gamma(\beta)})^{1-\beta}\frac{df(\varsigma)}{d\varsigma}.$

3. An analytical review for the non-linear beta-time fractional biological population model

Assuming the non-linear beta-time fractional biological population model equation given as follow:

$$\frac{\partial^{\beta} q}{\partial t^{\beta}} = \frac{\partial^2}{\partial x^2}(q^2) + \frac{\partial^2}{\partial y^2}(q^2) + \sigma(q^2-\rho). \tag{7}$$

Suppose the following wave transformations:

$$q(x,y,t)) = Q(\eta),\quad \eta = \theta x + \imath\theta y - \frac{\lambda}{\beta}(t+\frac{1}{\Gamma(\beta)})^{\beta}, \tag{8}$$

where θ and λ are parameters. Plugging Eq. (8) into Eq. (7), we get

$$\lambda Q' + \sigma Q^2 - \sigma\rho = 0. \tag{9}$$

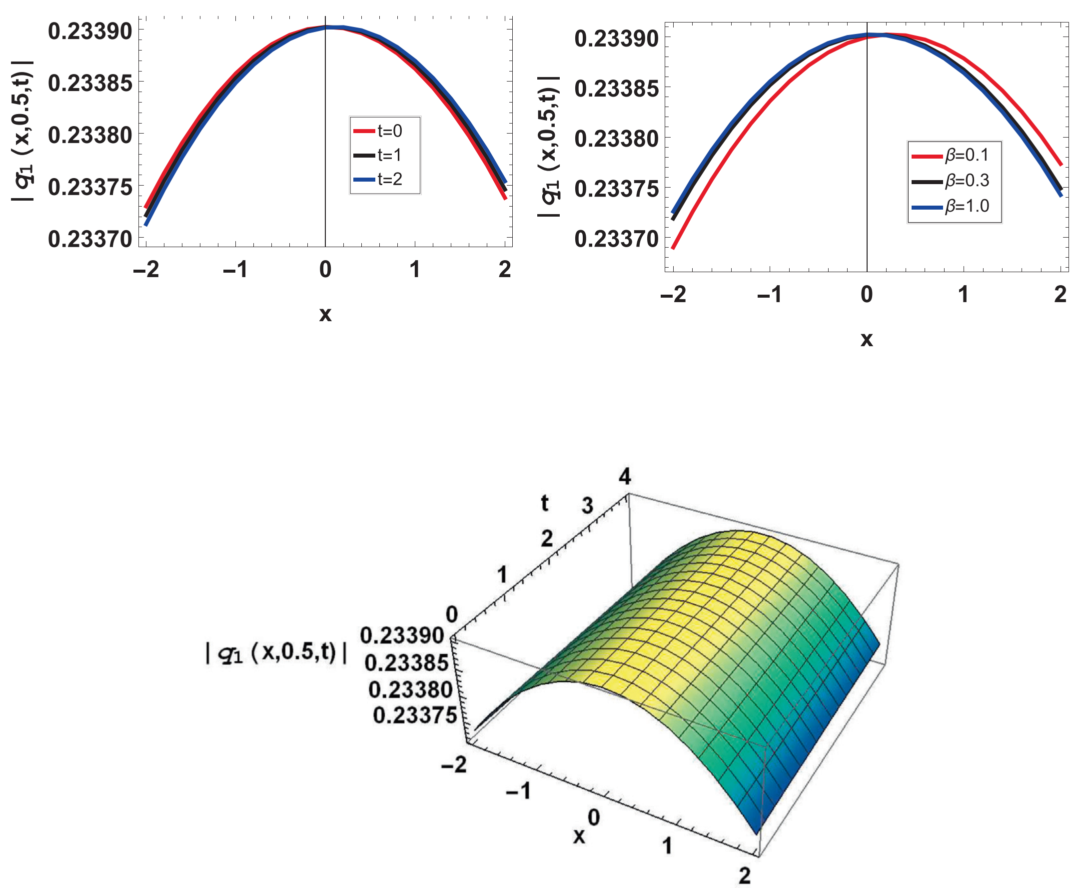

Fig. 1 Graph of set 1 for (25) at $\rho = 0.05, \sigma = 0.005, \theta = 0.09$.

4. Description of strategies

4.1. Explanation of the EShGEEM

The EShGEEM depends on the following steps:

Step 1: Consider the non-linear PDE:

$$Y(q, q^2 q_\gamma, q_\theta, q_{\theta\theta}, q_{\gamma\gamma}, q_{\gamma\theta}, \ldots) = 0, \quad (10)$$

where $q = q(\gamma, \theta)$. The next relation

$$q(\gamma, \theta) = Q(\eta), \quad \eta = \gamma - v\theta, \quad (11)$$

transform Eq. (10) to no-linear ODE given as:

$$F(Q, Q', Q', Q'', Q^2 Q', \ldots) = 0, \quad (12)$$

where F is a polynomial in its arguments.

Set 2: The solution of Eq. (12) has the general form:

$$Q(w) = \sum_{j=1}^{m} [\beta_j \sinh(w) + \alpha_j \cosh(w)]^j + \alpha_0. \quad (13)$$

The integer m, $m > 0$ in (13) can be obtained by the homogeneous balance condition on Eq. (12), α_0, α_j, β_j $(j = 1, 2, 3, \ldots, m)$ are constants, and w is a function determined by:

$$\frac{dw}{d\eta} = \sinh(w). \quad (14)$$

According to the [44], Eq. (14) solves to:

$$\sinh w(\eta) = \pm \text{csch}\eta \quad or \quad \cosh w(\eta) = \pm \coth \eta, \quad (15)$$

and

$$\sinh w(\eta) = \pm \imath \text{sech}\eta \quad or \quad \cosh w(\eta) = \pm \tanh \eta, \imath = \sqrt{-1}. \quad (16)$$

Step 3: Inserting Eqs. (13) and (14) into the Eq. (12) we gain new expressions in $w'^k(\eta) \sinh^l w(\eta) \cosh^m w(\eta)$ $(k = l = 0, 1, m = 0, 1, 2, \ldots)$. Next, equating the coefficients of $w'^k(\eta) \sinh^l w(\eta) \cosh^m w(\eta)$ to zero, we get different algebraic equations involving v, α_0, α_j and $\beta_j (j = 1, 2, 3, \ldots, m)$.

Step 4: By manipulating the above system with the aid of any computer package, we find the parameters v, α_0, α_j and β_j.

Step 5: Finally, we put back above values obtained in step 4 in Eqs. (15) and (16), we get the solutions of Eq. (12) in the form

$$Q(\eta) = \sum_{j=1}^{m} [\pm \imath \beta_j \text{sech}(\eta) \pm \alpha_j \tanh(\eta)]^j + \alpha_0, \quad (17)$$

and

$$Q(\eta) = \sum_{j=1}^{m} [\pm \beta_j \text{csch}(\eta) \pm \alpha_j \coth(\eta)]^j + \alpha_0. \quad (18)$$

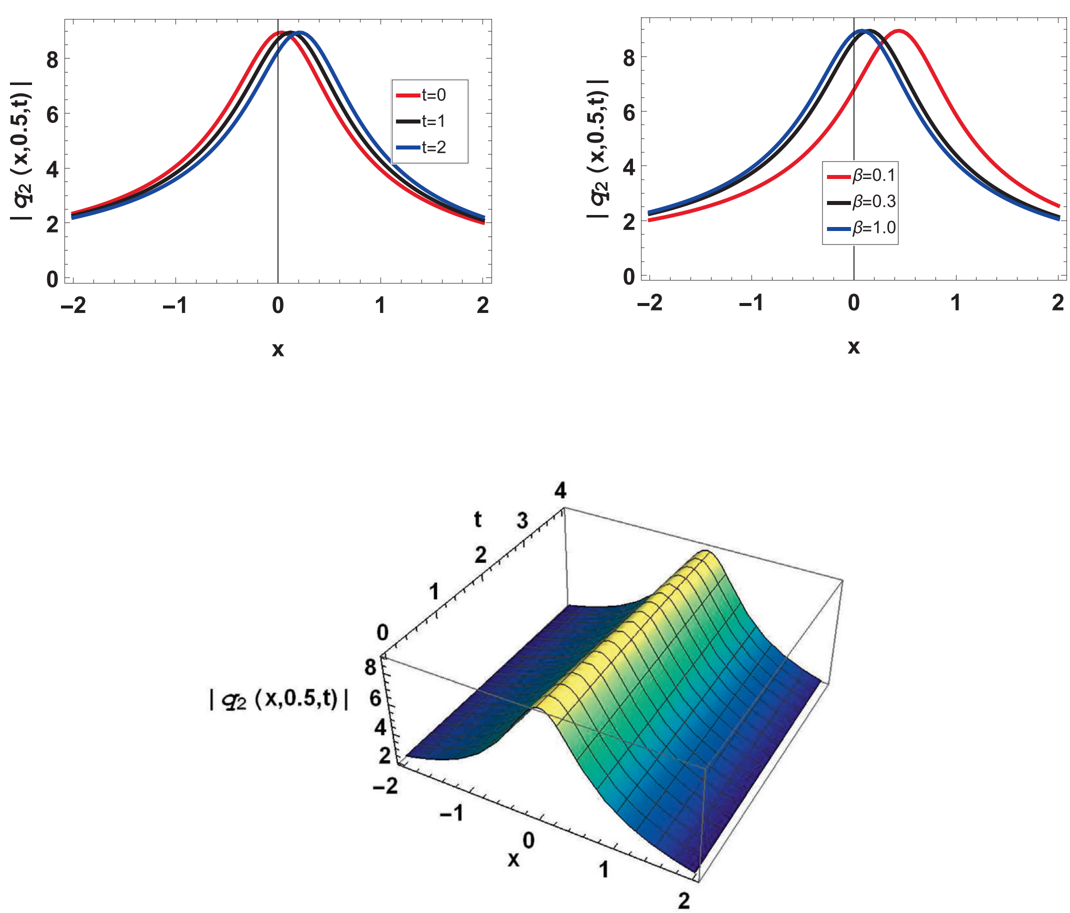

Fig. 2 Graph of set 2 for (29) at $\rho = 0.05, \sigma = 0.005, \theta = 0.09$.

4.2. Summary of Exp_a function method

Consider, the Eqs. (10)–(12). Let us suppose a solution of Eq. (12) is of the below type [46,47]:

$$Q(\eta) = \frac{a_0 + a_1 a^\eta + \ldots + a_m a^{m\eta}}{b_0 + b_1 a^\eta + \ldots + b_m a^{m\eta}}, \quad a \neq 0, 1, \tag{19}$$

here $a_j (0 \leqslant j \leqslant m)$ and $b_j (0 \leqslant j \leqslant m)$ are found later and m is obtained by the homogenous balance method in the presence of Eq. (12). Putting Eq. (19) into non-linear Eq. (12), yields

$$\wp(a^\eta) = \ell_0 + \ell_1 a^\eta + \ldots + \ell_t a^{t\eta} = 0. \tag{20}$$

Setting $\ell_j (0 \leqslant j \leqslant t)$ equal to zero, a system of algebraic equations is obtained and then we get non-trival solutions for the nonlinear PDE (10).

5. Analytical solutions via the EShGEEM

Using the homogenous balance condition on Eq. (9), we get $m = 1$. Thus, Eqs. (17), (18) and (13), respectively become:

$$Q(\eta) = \pm \imath \beta_1 \operatorname{sech}(\eta) \pm \alpha_1 \tanh(\eta) + \alpha_0, \tag{21}$$

$$Q(\eta) = \pm \beta_1 \operatorname{csch}(\eta) \pm \alpha_1 \coth(\eta) + \alpha_0, \tag{22}$$

$$Q(\eta) = \alpha_0 + \beta_1 \sinh(w) + \alpha_1 \cosh(w). \tag{23}$$

Plugging Eq. (23) into Eq. (9), we obtain a system of algebraic equations involved in the parameters $\alpha_0, \alpha_1 and \beta_1$ which solves to different solution sets:

Set 1:

$$\{\alpha_0 = 0, \alpha_1 = -\sqrt{\rho}, \beta_1 = -\sqrt{\rho}, \lambda = 2\sqrt{\rho}\sigma\}. \tag{24}$$

By using Eqs. (24) and (21), we obtain

$$q_1(x,y,t) = \sqrt{\rho}\Bigg(\imath \operatorname{sech}\left(\theta x + \imath\theta y - \frac{\lambda}{\beta}(t + \frac{1}{\Gamma(\beta)})^\beta\right) + \tanh\left(\theta x + \imath\theta y - \frac{\lambda}{\beta}(t + \frac{1}{\Gamma(\beta)})^\beta\right)\Bigg). \tag{25}$$

By using Eqs. (24) and (22), we procure

$$q_2(x,y,t) = \sqrt{\rho}\Bigg(\coth\left(\theta x + \imath\theta y - \frac{\lambda}{\beta}(t + \frac{1}{\Gamma(\beta)})^\beta\right) + \operatorname{csch}\left(\theta x + \imath\theta y - \frac{\lambda}{\beta}(t + \frac{1}{\Gamma(\beta)})^\beta\right)\Bigg). \tag{26}$$

Set 2:

$$\{\alpha_0 = 0, \alpha_1 = -\sqrt{\rho}, \beta_1 = \sqrt{\rho}, \lambda = 2\sqrt{\rho}\sigma\}. \tag{27}$$

By using Eqs. (27) and (21), we have

$$q_1(x,y,t) = \sqrt{\rho}\Bigg(-\imath \operatorname{sech}\left(\theta x + \imath\theta y - \frac{\lambda}{\beta}(t + \frac{1}{\Gamma(\beta)})^\beta\right) + \tanh\left(\theta x + \imath\theta y - \frac{\lambda}{\beta}(t + \frac{1}{\Gamma(\beta)})^\beta\right)\Bigg). \tag{28}$$

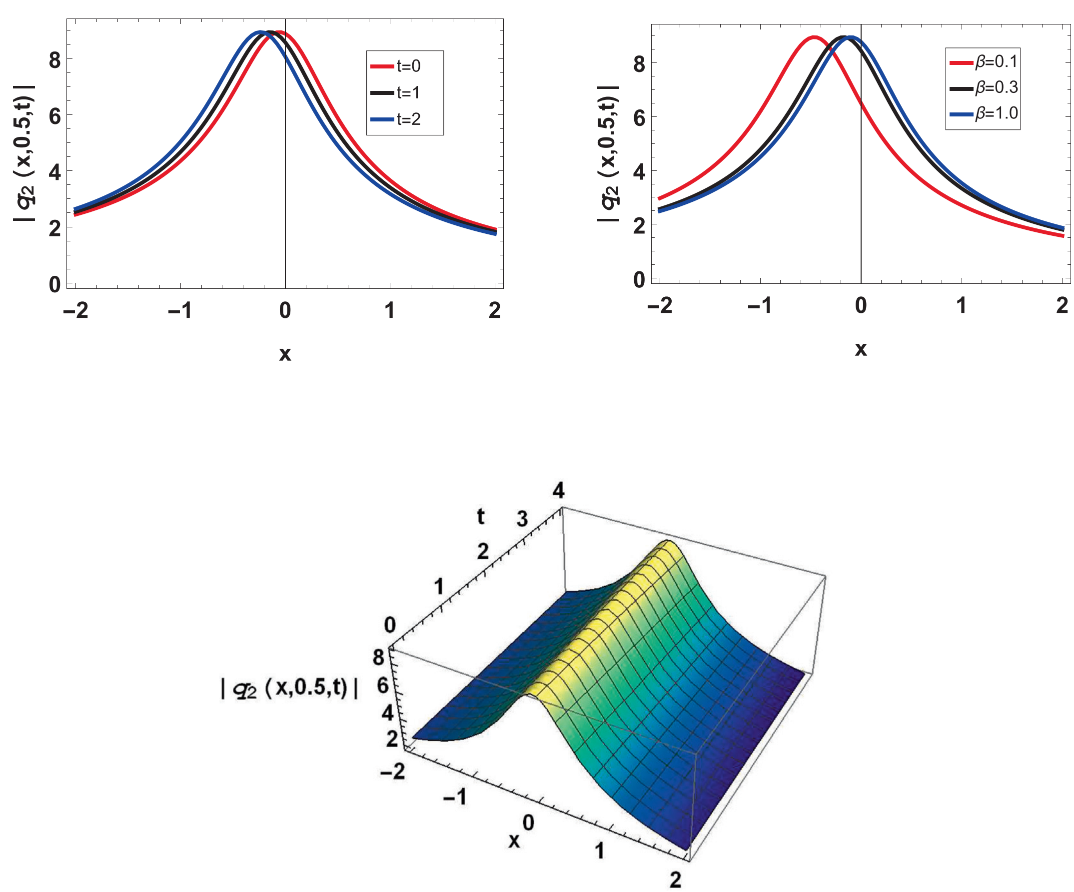

Fig. 3 Graph of set 3 for (32) at $\rho = 0.05, \sigma = 0.005, \theta = 0.09$.

By using Eqs. (27) and (22), we attain

$$q_2(x,y,t) = \sqrt{\rho}\Big(-\mathrm{csch}\Big(\theta x + \imath\theta y - \frac{\lambda}{\beta}(t + \frac{1}{\Gamma(\beta)})^{\beta}\Big) + \coth\Big(\theta x + \imath\theta y - \frac{\lambda}{\beta}(t + \frac{1}{\Gamma(\beta)})^{\beta}\Big)\Big). \quad (29)$$

Set 3:

$$\{\alpha_0 = 0, \alpha_1 = \sqrt{\rho}, \beta_1 = -\sqrt{\rho}, \lambda = -2\sqrt{\rho\sigma}\}. \quad (30)$$

Eqs. (30) and (21) yield

$$q_1(x,y,t) = \sqrt{\rho}\Big(\imath\mathrm{sech}\Big(\theta x + \imath\theta y - \frac{\lambda}{\beta}(t + \frac{1}{\Gamma(\beta)})^{\beta}\Big) - \tanh\Big(\theta x + \imath\theta y - \frac{\lambda}{\beta}(t + \frac{1}{\Gamma(\beta)})^{\beta}\Big)\Big). \quad (31)$$

By using Eqs. (31) and (22), we gather

$$q_2(x,y,t) = \sqrt{\rho}\Big(\mathrm{csch}\Big(\theta x + \imath\theta y - \frac{\lambda}{\beta}(t + \frac{1}{\Gamma(\beta)})^{\beta}\Big) - \coth\Big(\theta x + \imath\theta y - \frac{\lambda}{\beta}(t + \frac{1}{\Gamma(\beta)})^{\beta}\Big)\Big). \quad (32)$$

Set 4:

$$\{\alpha_0 = 0, \alpha_1 = \sqrt{\rho}, \beta_1 = \sqrt{\rho}, \lambda = -2\sqrt{\rho\sigma}\}. \quad (33)$$

By using Eqs. (33) and (21), we attain

$$q_1(x,y,t) = -\sqrt{\rho}\Big(\imath\mathrm{sech}\Big(\theta x + \imath\theta y - \frac{\lambda}{\beta}(t + \frac{1}{\Gamma(\beta)})^{\beta}\Big) + \tanh\Big(\theta x + \imath\theta y - \frac{\lambda}{\beta}(t + \frac{1}{\Gamma(\beta)})^{\beta}\Big)\Big). \quad (34)$$

Eqs. (33) and (22) yield

$$q_2(x,y,t) = -\sqrt{\rho}\Big(\coth\Big(\theta x + \imath\theta y - \frac{\lambda}{\beta}(t + \frac{1}{\Gamma(\beta)})^{\beta}\Big) + \mathrm{csch}\Big(\theta x + \imath\theta y - \frac{\lambda}{\beta}(t + \frac{1}{\Gamma(\beta)})^{\beta}\Big)\Big). \quad (35)$$

Set 5:

$$\{\alpha_0 = 0, \alpha_1 = -\sqrt{\rho}, \beta_1 = 0, \lambda = \sqrt{\rho\sigma}\}. \quad (36)$$

By using Eqs. (36) and (21), we gain

$$q_1(x,y,t) = \sqrt{\rho}\tanh\Big(\theta x + \imath\theta y - \frac{\lambda}{\beta}(t + \frac{1}{\Gamma(\beta)})^{\beta}\Big). \quad (37)$$

Eqs. (36) and (22), yield

$$q_2(x,y,t) = \sqrt{\rho}\coth\Big(\theta x + \imath\theta y - \frac{\lambda}{\beta}(t + \frac{1}{\Gamma(\beta)})^{\beta}\Big). \quad (38)$$

Set 6:

$$\{\alpha_0 = 0, \alpha_1 = \sqrt{\rho}, \beta_1 = 0, \lambda = -\sqrt{\rho\sigma}\}. \quad (39)$$

Now using Eqs. (39) and (21) yield

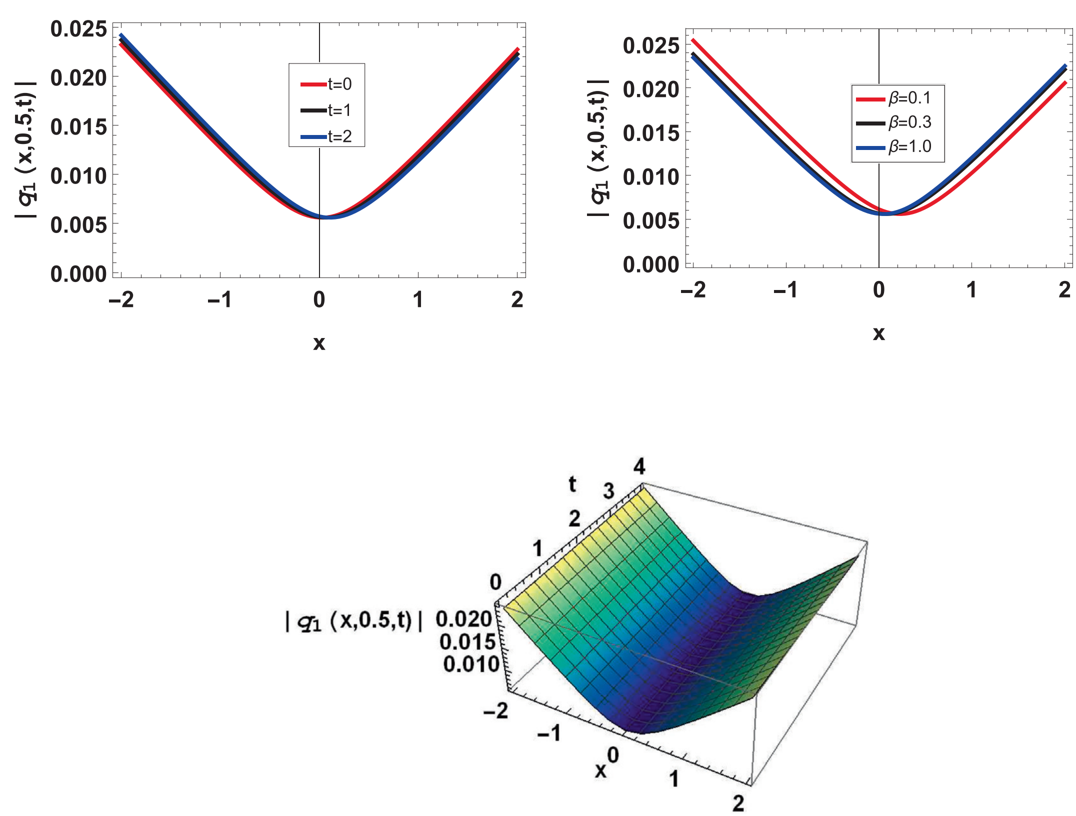

Fig. 4 Graph of set 5 for (37) at $\rho = 0.05, \sigma = 0.005, \theta = 0.09$.

$$q_1(x,y,t)=\sqrt{\rho}\tanh\left(\theta x+\iota\theta y-\frac{\lambda}{\beta}\left(t+\frac{1}{\Gamma(\beta)}\right)^{\beta}\right). \tag{40}$$

By using Eqs. (39) and (22), we secure

$$q_2(x,y,t)=\sqrt{\rho}\coth\left(\theta x+\iota\theta y-\frac{\lambda}{\beta}\left(t+\frac{1}{\Gamma(\beta)}\right)^{\beta}\right). \tag{41}$$

6. Analytical solutions via the Exp_a function method

By applying the homogenous balance condition on Eq. (9), we find that $m=1$. Thus, Eq. (19) takes the form:

$$Q(\eta)=\frac{a_0+a_1a^{\eta}}{b_0+b_1a^{\eta}}. \tag{42}$$

Placing the above equation in Eq. (9) and solving, we secure the solution sets given below.

Set 1:

$$\left\{a_0=-\sqrt{\rho}b_0, a_1=\sqrt{\rho}b_1, \lambda=\frac{2\sqrt{\rho}\sigma}{\log(a)}\right\}. \tag{43}$$

By using Eqs. (42) and (43), we secure the following solutions,

$$q_1(x,y,t)=-\sqrt{\rho}\left(\frac{b_0-b_1a^{\theta x+\iota\theta y-\frac{\lambda}{\beta}(t+\frac{1}{\Gamma(\beta)})^{\beta}}}{b_0+b_1a^{\theta x+\iota\theta y-\frac{\lambda}{\beta}(t+\frac{1}{\Gamma(\beta)})^{\beta}}}\right). \tag{44}$$

Set 2:

$$\left\{a_0=\sqrt{\rho}b_0, a_1=-\sqrt{\rho}b_1, \lambda=-\frac{2\sqrt{\rho}\sigma}{\log(a)}\right\}. \tag{45}$$

Eqs. (44) and (45) imply,

$$q_2(x,y,t)=\sqrt{\rho}\left(\frac{b_0-b_1a^{\theta x+\iota\theta y-\frac{\lambda}{\beta}(t+\frac{1}{\Gamma(\beta)})^{\beta}}}{b_0+b_1a^{\theta x+\iota\theta y-\frac{\lambda}{\beta}(t+\frac{1}{\Gamma(\beta)})^{\beta}}}\right). \tag{46}$$

7. Finite difference scheme

The finite difference scheme gives the approximation of q_x, q_{xx}, q_y and q_{yy} as [54]:

$$\begin{aligned} q_x &\simeq \frac{\vartheta_{i+1,j,n}-\vartheta_{i-1,j,n}}{2h}, \\ q_{xx} &\simeq \frac{\vartheta_{i-1,j,n}+\vartheta_{i+1,j,n}-2\vartheta_{i,j,n}}{h^2}, \\ q_y &\simeq \frac{\vartheta_{i,j+1,n}-\vartheta_{i,j-1,n}}{2k}, \\ q_{yy} &\simeq \frac{\vartheta_{i,j-1,n}+\vartheta_{i,j+1,n}-2\vartheta_{i,j,n}}{k^2}. \end{aligned} \tag{47}$$

From the conformal fractional derivative, we have:

If $0<\beta\leqslant 1$ and the function q is β differentiable when $t>0$, then

$$\frac{\partial^{\beta}q}{\partial t^{\beta}}=\left(t+\frac{1}{\Gamma(\beta)}\right)^{1-\beta}\frac{dq(t)}{dt}. \tag{48}$$

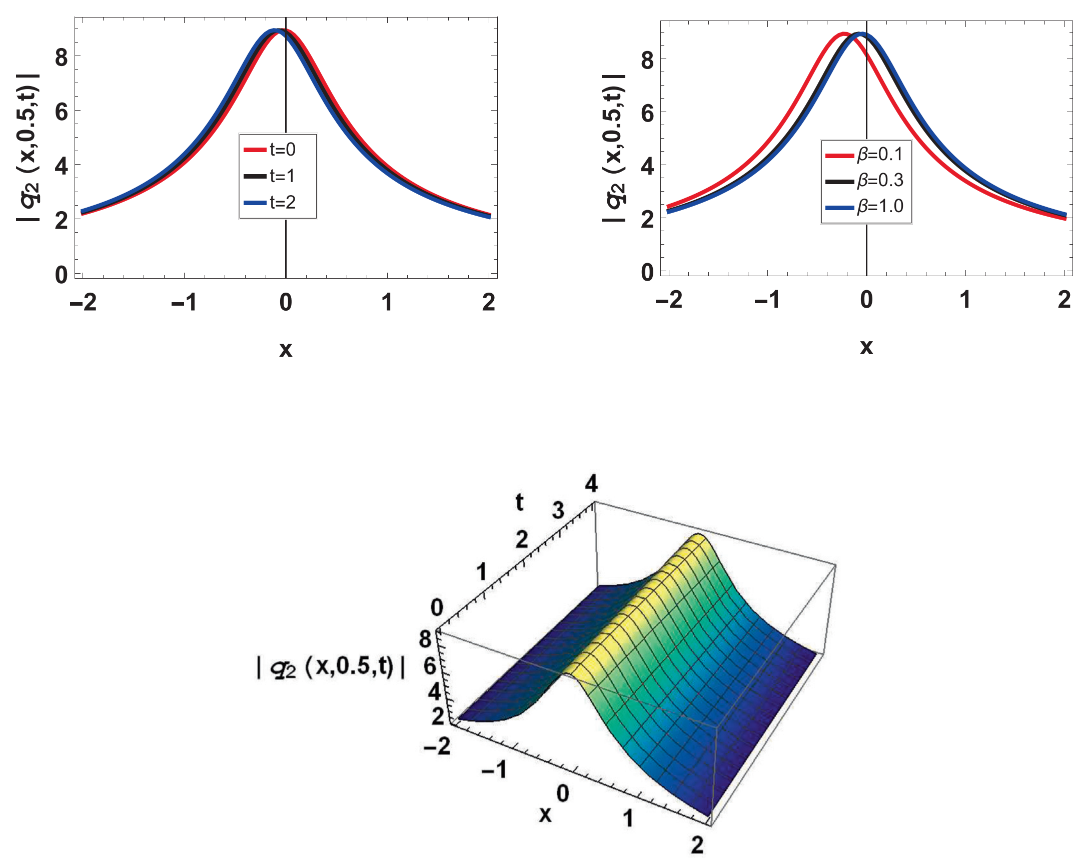

Fig. 5 Graph of set 6 for (41) at $\rho=0.05, \sigma=0.005, \theta=0.09$.

Also, the approximations for q_t via the finite difference scheme is given by [54]

$$q_t \simeq \frac{\vartheta_{i,j,n+1} - \vartheta_{i,j,n}}{\Delta t}. \tag{49}$$

From (48) and (49) we get

$$\frac{\partial^\beta q}{\partial t^\beta} \simeq \left(t + \frac{1}{\Gamma(\beta)}\right)^{1-\beta} \frac{\vartheta_{i,j,n+1} - \vartheta_{i,j,n}}{\Delta t}. \tag{50}$$

For an exact solution q at a grid point $G_i = G_i(x_i, y_j, t_n)$, we assume that $\vartheta_{i,j,n}$ is the numerical solution at G_i. Substituting (47) and (50) into (6), we get

$$\begin{aligned}&\left(t_n + \tfrac{1}{\Gamma(\beta)}\right)^{1-\beta} \tfrac{\vartheta_{i,j,n+1}-\vartheta_{i,j,n}}{\Delta t} - 2\left(\tfrac{\vartheta_{i+1,j,n}-\vartheta_{i-1,j,n}}{2h}\right)^2 - \\ &2\vartheta_{i,j,n}\left(\tfrac{\vartheta_{i-1,j,n}+\vartheta_{i+1,j,n}-2\vartheta_{i,j,n}}{h^2}\right) - 2\left(\tfrac{\vartheta_{i,j+1,n}-\vartheta_{i,j-1,n}}{2k}\right)^2 - \\ &2\vartheta_{i,j,n}\left(\tfrac{\vartheta_{i,j-1,n}+\vartheta_{i,j+1,n}-2\vartheta_{i,j,n}}{k^2}\right) - \sigma(\vartheta^2_{i,j,n} - \rho) = 0.\end{aligned} \tag{51}$$

7.1. The numerical outcomes

In this section, we introduce some numerical outcomes for the nonlinear biological population model (See Tables 1–4).

8. Graphical illustration and applications

In this part, some figures in 2D and 3D are depicted to investigate some analytical and numerical solutions for Eq. (6). Figs. 1–7 show the analytical solutions given by Eqs. (25), (29), (32), (37), (41), (44) and (46), respectively. While the 2D Figs. 8 and 9 show the accuracy of the numerical outcomes compared to the analytical solutions given by Eqs. (25) and (44), respectively.

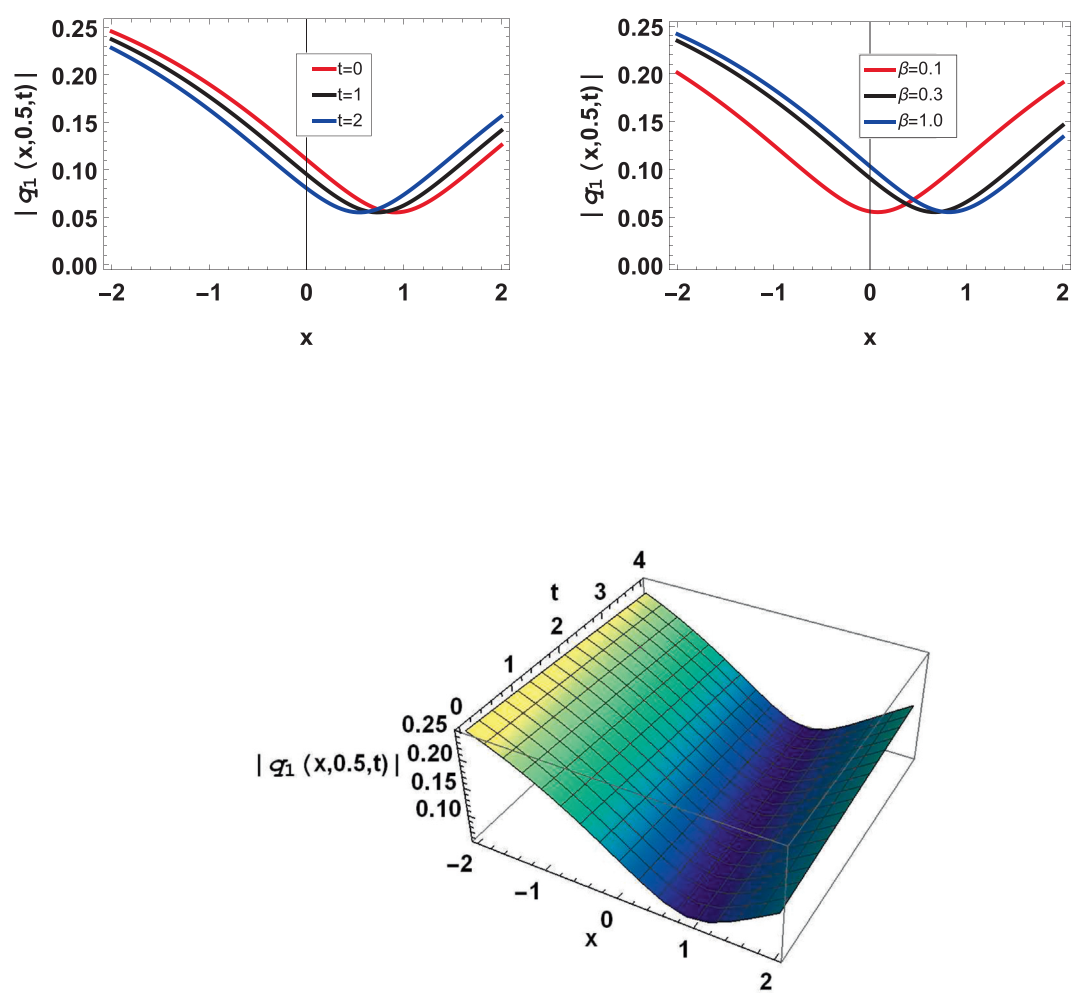

Fig. 6 Graph of set 1 for (44) at $b_0 = 0.01, b_1 = 0.02, a = 0.1, \rho = 0.1, \sigma = 0.1, \theta = 0.3$.

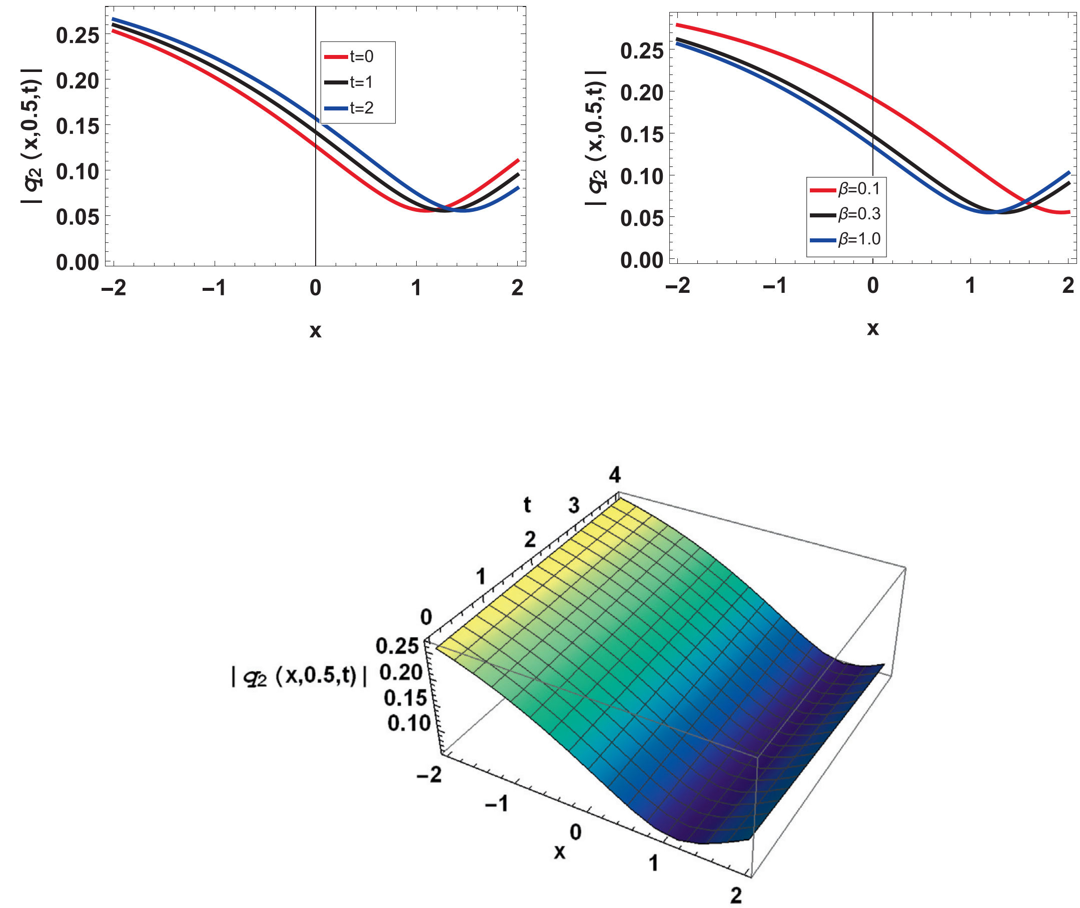

Fig. 7 Graph of set 1 for (46) at $b_0 = 0.01, b_1 = 0.02, a = 0.1, \rho = 0.1, \sigma = 0.1, \theta = 0.3$.

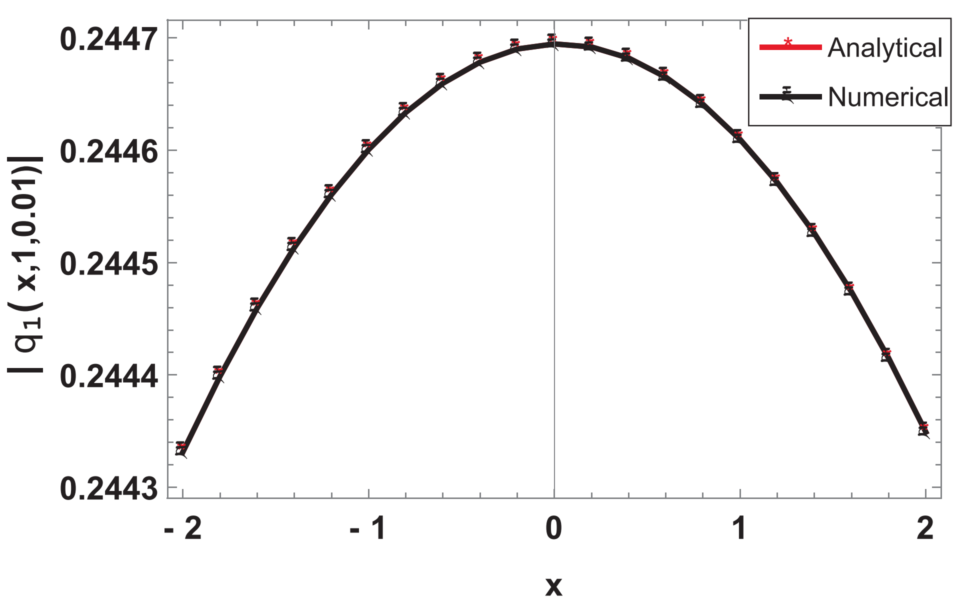

Fig. 8 Graph of analytical and numerical solutions given by Table 1.

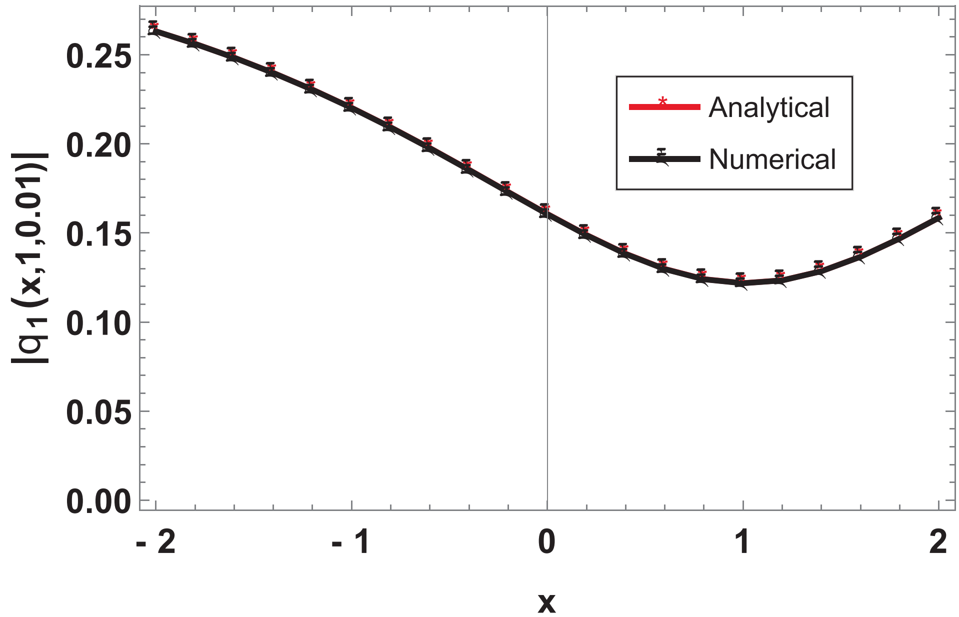

Fig. 9 Graph of analytical and numerical solutions given by Table 3.

9. Conclusion

The current study has dealt with different types of solitary wave solutions for biological population model with novel beta-time derivative operators. This new form of the aforesaid classical model has been constructed for its new soliton solutions via the EShGEEM and the Exp_a function method. The solutions showed that these methods have the ability to producing a variety of solitary waves and other solutions to fractional differential equations. In particular, the dark, bright and singular solitons and other solutions have procured. Also, we have obtained the numerical solution for the beta-time fractional biological population model equation based on the finite difference method. Thus, the obtained results helpful in describing the biological population model in some better way with numerical simulations. Moreover, the validity of our achieved numerical solutions will give power support to the obtained exact solutions (the powerful of the obtained numerical solutions relative to its initial conditions are extracted from the obtained exact solutions). As a result, a positive outlook for future studies has been developed for the given model.

Funding

None.

Declaration of Competing Interest

The authors declare that they have no known competing financial interests or personal relationships that could have appeared to influence the work reported in this paper.

References

[1] S. Bentout, S. Djilali, S. Kumar, Mathematical analysis of the influence of prey escaping from prey herd on three species fractional predator-prey interaction model, Phys. A 572 (2021) 125840.
[2] S. Djilali, S. Bentout, B. Ghanbari, S. Kumar, Spatial patterns in a vegetation model with internal competition and feedback regulation, Eur. Phys. J. Plus 136 (2021) 256.
[3] S. Bentout, Y. Chen, S. Djilali, Global dynamics of an SEIR model with two age structures and a nonlinear incidence, Acta Appl. Math. 171 (2021) 7.
[4] S. Bentout, S. Djilali, A. Chekroun, Global threshold dynamics of an age structured alcoholism model, Int. J. Biomath. (2020), https://doi.org/10.1142/S1793524521500133.
[5] A. Biswas, R.T. Alqahtani, Chirp-free bright optical solitons for perturbed Gerdjikov-Ivanov equation by semi-inverse variational principle, Optik 147 (2017) 72–76.
[6] A. Bekir, Applications of the extended tanh method for coupled nonlinear evolution equations, Commun. Nonlinear Sci. 13 (9) (2008) 1748–1757.
[7] M.S. Osman, H.I. Abdel-Gawad, M.A. El Mahdy, Two-layer-atmospheric blocking in a medium with high nonlinearity and lateral dispersion, Result phys. 8 (2018) 1054–1060.
[8] H.I. Abdel-Gawad, M. Osman, On shallow water waves in a medium with time-dependent dispersion and nonlinearity coefficients, J. Adv. Res. 6 (4) (2015) 593–599.
[9] M.S. Osman, Multi-soliton rational solutions for some nonlinear evolution equations, Open Phys. 14 (1) (2016) 26–36.
[10] M.S. Osman, Multi-soliton rational solutions for quantum Zakharov-Kuznetsov equation in quantum magnetoplasmas, Wave Random Complex 26 (4) (2016) 434–443.
[11] M.S. Osman, D. Baleanu, A.R. Adem, K. Hosseini, M. Mirzazadeh, M. Eslami, Double-wave solutions and Lie symmetry analysis to the (2 + 1)-dimensional coupled Burgers equations, Chin. J. Phys. 63 (2020) 122–129.

[12] H.F. Ismael HF, H. Bulut, C. Park, M.S. Osman, M-Lump, N-soliton solutions, and the collision phenomena for the (2+ 1)-dimensional Date-Jimbo-Kashiwara-Miwa equation, Result. Phys. 19 (2020) 103329.
[13] J.H. He, Variational principle and periodic solution of the Kundu-Mukherjee-Naskar equation, Results Phys. 17 (2020) 103031.
[14] Y. Yíldírím, M. Mirzazadeh, Optical pulses with Kundu-Mukherjee-Naskar model in fiber communication systems, Chin. J. Phys. 64 (2020) 183–193.
[15] M. Aljahdali, A.A. El-Sherif, Equilibrium studies of binary and mixed-ligand complexes of zinc (II) involving 2-(aminomethyl)-benzimidazole and some bio-relevant ligands, J. Solution Chem. 41 (10) (2012) 1759–1776.
[16] K.K. Ali, A.M. Wazwaz, M.S. Mehanna, M.S. Osman, On short-range pulse propagation described by (2+ 1)-dimensional Schrödinger's hyperbolic equation in nonlinear optical fibers, Phys. Scr. 95 (7) (2020) 075203.
[17] H. Bulut, T.A. Sulaiman, F. Erdogan, H.M. Baskonus, On the new hyperbolic and trigonometric structures to the simplified MCH and SRLW equations, Eur. Phys. J. Plus 132 (2017) 350.
[18] H.M. Baskonus, T.A. Sulaiman, H. Bulut, New solitary wave solutions to the (2+ 1)-dimensional Calogero-Bogoyavlenskii-Schiff and the Kadomtsev-Petviashvili hierarchy equations, Indian, J. Phys. 91 (10) (2017) 1237–1243.
[19] M.S. Osman, H. Rezazadeh, M. Eslami, A. Neirameh, M. Mirzazadeh, Analytical study of solitons to benjamin-bona-mahony-peregrine equation with power law nonlinearity by using three methods, U. Politeh. Buch. Ser. A 80 (4) (2018) 267–278.
[20] S. Kumar, A. Kumar, B. Samet, J.F. Gómez-Aguilar, M.S. Osman, A chaos study of tumor and effector cells in fractional tumor-immune model for cancer treatment, Chaos Soliton. Fract. 141 (2020) 110321.
[21] K.K. Ali, A.R. Hadhoud, New solitary wave solutions of a highly dispersive physical model, Results Phys. 17 (2020) 103137.
[22] F.S. Bayones, K.S. Nisar, K.A. Khan, N. Raza, N.S. Hussien, M.S. Osman, K.M. Abualnaja, Magneto-hydrodynamics (MHD) flow analysis with mixed convection moves through a stretching surface, AIP Adv. 11 (4) (2021) 045001.
[23] M.O. Al-Amr, H. Rezazadeh, K.K. Ali, A. Korkmazki, N1-soliton solution for Schrödinger equation with competing weakly nonlocal and parabolic law nonlinearities, Commun. Theor. Phys. 72 (6) (2020) 065503.
[24] S. Dhawan, J.A.T. Machado, D.W. Brzeziński, M.S. Osman, A Chebyshev Wavelet Collocation Method for Some Types of Differential Problems, Symmetry 13 (4) (2021) 536.
[25] J.G. Liu, M.S. Osman, A.M. Wazwaz, A variety of nonautonomous complex wave solutions for the (2+ 1)-dimensional nonlinear Schrödinger equation with variable coefficients in nonlinear optical fibers, Optik 180 (2019) 917–923.
[26] K.K. Ali, C. Cattani, J.F. Gómez-Aguilar, D. Baleanu, M.S. Osman, Analytical and numerical study of the DNA dynamics arising in oscillator-chain of Peyrard-Bishop model, Chaos Soliton. Fract. 139 (2020) 110089.
[27] G. Yel, H.M. Baskonus, H. Bulut, Novel archetypes of new coupled Konno-Oono equation by using sine-Gordon expansion method, Opt. Quant. Electron. 49 (2017) 285.
[28] H.M. Baskonus, H. Bulut, T.A. Sulaiman, Investigation of various travelling wave solutions to the extended (2+ 1)-dimensional quantum ZK equation, Eur. Phys. J. Plus 132 (2017) 482.
[29] K.K. Ali, A.M. Wazwaz, M.S. Osman, Optical soliton solutions to the generalized nonautonomous nonlinear Schrödinger equations in optical fibers via the sine-Gordon expansion method, Optik 208 (2020) 164132.
[30] A.A. El-Sherif, M.M. Shoukry, Equilibrium investigation of complex formation reactions involving copper (II), nitrilo-tris (methyl phosphonic acid) and amino acids, peptides or DNA constitutents. The kinetics, mechanism and correlation of rates with complex stability for metal ion promoted hydrolysis of glycine methyl ester, J. Coord. Chem. 59 (14) (2006) 1541–1556.
[31] S. Djilali, S. Bentout, Spatiotemporal patterns in a diffusive predator-prey model with prey social behavior, Acta Appl. Math. 169 (2020) 125–143.
[32] S. Bentout, B. Ghanbari, S. Djilali, L. Narayan Guin, Impact of predation in the spread of an infectious disease with time fractional derivative and social behavior, Int. J. Model. Simul. Sci. Comput. (2020), https://doi.org/10.1142/S1793962321500239.
[33] S. Djilali, B. Ghanbari, S. Bentout, A. Mezouaghi, Turing-Hopf bifurcation in a diffusive mussel-algae model with time-fractional-order derivative, Chaos Soliton. Fract. 138 (2020) 109954.
[34] S. Djilali, T.M. Touaoula, S.E.H. Miri, A heroin epidemic model: very general non linear incidence, treat-age, and global stability, Acta Appl. Math. 152 (2017) 171–194.
[35] M.E. Gurtin, R.C. MacCamy, On the diffusion of biological populations, Math. Biosci. 33 (1–2) (1977) 35–49.
[36] W.S. Gurney, R.M. Nisbet, The regulation of inhomogeneous populations, J. Theor. Biol. 52 (2) (1975) 441–457.
[37] Ö. Güner, A. Bekir, A novel method for nonlinear fractional differential equations using symbolic computation, Waves Random Complex Med. 27 (1) (2017) 163–170.
[38] Y.G. Lu, Hölder estimates of solutions of biological population equations, Appl. Math. Lett. 13 (6) (2000) 123–126.
[39] A. Bekir, Ö Güner, A.C. Cevikel, Fractional complex transform and exp-function methods for fractional differential equations, Abstr. Appl. Anal. 2013 (2013). Article ID 426462. Hindawi.
[40] A. Bekir A, Ö Güner, Exact solutions of nonlinear fractional differential equations by (G'/G)-expansion method, Chin. Phys. B 22 (11) (2013) 110202.
[41] S.T. Mohyud-Din, A. Ali, B. Bin-Mohsin, On biological population model of fractional order, Int. J. Biomath. 9 (05) (2016) 1650070.
[42] A.M. El-Sayed, S.Z. Rida, A.A. Arafa, Exact solutions of fractional-order biological population model, Commun. Theor. Phys. 52 (6) (2009) 992.
[43] M. Shakeel, M.A. Iqbal, S.T. Mohyud-Din, Closed form solutions for nonlinear biological population model, J. Biol. Syst. 26 (01) (2–18) 207–223..
[44] Y. Xian-Lin, T. Jia-Shi, Travelling wave solutions for Konopelchenko-Dubrovsky equation using an extended sinh-Gordon equation expansion method, Commun. Theor. Phys. 50 (5) (2008) 1047.
[45] H. Bulut, T.A. Sulaiman, H.M. Baskonus, H. Rezazadeh, M. Eslami, M. Mirzazadeh, Optical solitons and other solutions to the conformable space-time fractional Fokas-Lenells equation, Optik 172 (2018) 20–27.
[46] A.T. Ali, E.R. Hassan, General Exp_a-function method for nonlinear evolution equations, Appl. Math. Comput. 217 (2) (2010) 451–459.
[47] A. AZafar, A. Bekir, M. Raheel, H. Rezazadeh, Investigation for Optical Soliton Solutions of Two Nonlinear Schrödinger Equations via Two Concrete Finite Series Methods, Int. J. Appl. Comput. Math. 6 (2020) 1–3.
[48] A. Atangana, D. Baleanu, A. Alsaedi, Analysis of time-fractional Hunter-Saxton equation: a model of neumatic liquid crystal, Open Phys. 14 (1) (2016) 145–149.
[49] A. Atangana, R.T. Alqahtani, Modelling the spread of river blindness disease via the caputo fractional derivative and the beta-derivative, Entropy 18 (2) (2016) 40.

[50] H. Yépez-Martinez, J.F. Gómez-Aguilar, D. Baleanu, Beta-derivative and sub-equation method applied to the optical solitons in medium with parabolic law nonlinearity and higher order dispersion, Optik 155 (2018) 357–365.
[51] A. Yusuf, M. Inc, A.I. Aliyu, D. Baleanu, Optical solitons possessing beta derivative of the Chen-Lee-Liu equation in optical fibers, Front. Phys. 7 (2019) 34.
[52] M.F. Uddin, M.G. Hafez, Z. Hammouch, D. Baleanu, Periodic and rogue waves for Heisenberg models of ferromagnetic spin chains with fractional beta derivative evolution and obliqueness, Wave. Random Complex (2020), https://doi.org/10.1080/17455030.2020.1722331.
[53] B. Ghanbari, J.F. Gómez-Aguilar, The generalized exponential rational function method for Radhakrishnan-Kundu-Lakshmanan equation with β-conformable time derivative, Rev. Mex. Fis. 65 (5) (2019) 503–518.
[54] K.R. Raslan, K.K. Ali, Numerical study of MHD-duct flow using the two-dimensional finite difference method, Appl. Math. Inf. Sci. 14 (4) (2020) 17.